Numerical Modeling and Experimental Study of the Frontal Polymerization of the Diglycidyl Ether of Bisphenol A/Diethylenetriamine Epoxy System

E. Frulloni,[1] M. M. Salinas,[1] L. Torre,[1] A. Mariani,[2] J. M. Kenny[1]

[1]*Material Science and Technology Center, University of Perugia, Perugia, Italy*
[2]*Dipartimento di Chimica, Università di Sassari and local Consorzio Interuniversitario Nazionale per la Scienza e Tecnologia dei Materiali (INSTM) research unit, Via Vienna 2, 07100 Sassari, Italy*

Received 21 June 2004; accepted 13 August 2004
DOI 10.1002/app.21644
Published online in Wiley InterScience (www.interscience.wiley.com).

ABSTRACT: Frontal polymerization is a process in which a spatially localized reaction zone propagates through a monomer by converting it into a polymer. In particular, the heat produced during the curing process is exploited to promote the reaction of the monomer lying next to the propagating front, making this latter able to self-sustain. This approach represents an alternative solution to traditional polymerization methods and can be successfully applied to the preparation of many polymeric materials. In this study, frontal polymerization was numerically modeled to better understand it and to provide the basis for processing simulation. A finite-difference method was used to solve the thermal problem coupled with the equation describing the cure evolution for a reactor with a cylindrical geometry. The implicit backward time–centered space method was used. First, a one-dimensional model, able to describe the process in an adiabatic tube, was developed. The front ignition was simulated as if it were a hot surface warming one end of the reactor to trigger reactant polymerization. The model was able to predict the formation of a reactive front advancing in the unreacted zone with a constant speed. The influence of the chemical and physical properties of the resin on process evolution was also investigated. By applying the alternate direction implicit method, a more detailed two-dimensional model able to describe a three-dimensional problem for a cylindrical reactor was also developed. With this model, it was possible to study the influence of boundary conditions on process evolution, considering a convective heat exchange with the environment through the reactor walls. Diglycidyl ether of bisphenol A, cured with diethylenetriamine (DETA), was used as the model system. Differential scanning calorimetry was used to produce a phenomenological model able to describe the cure process and to determine the physical properties of the resin. The validity of the approach was confirmed experimentally using a small cylindrical reactor. J Appl Polym Sci 96: 1756–1766, 2005

Key words: frontal polymerization; modeling; reactive processing; differential scanning calorimetry (DSC); resins

INTRODUCTION

In frontal polymerization (FP) a spatially localized reaction zone propagates through a monomer, thus converting it into a polymer. This approach represents an alternative solution to traditional polymerization techniques and has been successfully applied to production of poly-ε-caprolactam,[1] polyacrylates,[2] epoxy resins[3–7] and their interpenetrating polymer networks (IPNs) with polyacrylates,[8] polyurethanes,[9,10] polydicyclopentadiene[11] and its IPNs with polyacrylates,[12] and unsaturated polyester resins.[13,14] Recently, thiolene chemistry[15] and atom transfer radical polymerization[16] were also used in FP. The macrokinetics and dynamics of FP were thoroughly studied by Pojman et al.[8,17–20] The FP process was also simulated by Apostolo et al.[21] and by Spade and Volpert.[22]

In classical bulk polymerizations, heat is uniformly provided during the entire cure cycle to the whole surface of the reactive monomers, thus promoting their reaction. Conversely, during FP heat is applied to a small area of the sample and for a time interval that is short if compared with the total cure time for the sample. The local increase in temperature triggers the polymerization of the monomers (or reactants) within the heating region of interest and the heat released by the curing process is transferred to the surroundings, promoting the creation of a hot reaction front that propagates in the rest of the monomers, thus converting them into polymer.

FP presents many advantages with respect to bulk processes, although sometimes it may be more complex and difficult to control. Indeed, smaller amounts of energy are needed to carry out the process and, even for resin systems that exhibit a diffusion-con-

Correspondence to: J. M. Kenny (kenny@unipg.it).

TABLE I
Physical Properties Measured for the Resin

Parameter	Value
Density ρ, kg/m^3	1.19
Thermal conductivity k, W/m^{-1}/K^{-1}	0.19
Specific heat C_p, J/kg^{-1}/K^{-1}	
At T = 30°C	2230
At T = 140°C	3118

trolled curing process,[23] FP often yields products with a higher degree of cure.[7,13,14] Although in the case of bulk polymerization the reaction is controlled by the reactor temperature, in that of FP, the reaction process is mainly governed by the chemical and physical properties of the reacting system. Front velocity and front temperature are strictly dependent on the enthalpy of the cure reaction, on the reaction kinetics, on the thermal conductivity of the resin, and on the resin heat capacity. Because front polymerization is a dynamic phenomenon and there are many variables that can influence it, a numerical simulation of the whole process can help in the investigation of the influence of the various parameters and in process optimization.

EXPERIMENTAL

As the experimental system to be modeled, the epoxy resin, obtained by the reaction of 7.2 parts in weight of diglycidyl ether of bisphenol A (DGEBA; M_n of 377) and 1.0 part in weight of diethylenetriamine (DETA), was used. Both resin components were supplied by Sigma-Aldrich (Milan, Italy) and were used as received. The development of the reaction kinetics and the determination of the thermal properties of the resin were performed using a DSC apparatus (Mettler Toledo International, Zurich, Switzerland), through dynamical and isothermal scans at various temperatures. From the dynamic test that was performed within a temperature range of −50 to +180°C and with a heating rate of 20°C/min, a total heat of reaction of 550 J/g was found. The glass-transition temperature of the fully cured resin was 125°C. The reaction onset of the mixture was around 40°C, whereas the exothermic peak was reached at 100°C. With these indications, temperatures between 50 and 80°C were chosen to perform the isothermal tests that were used for the characterization of the reaction kinetics.

The main physical properties of the resin, necessary to describe the problem, were measured and are summarized in Table I. Density was measured using a Mettler balance provided with a density evaluation kit and DSC was used for thermal conductivity. Heat capacity was evaluated using the method described in Turi[24] and the measurements were carried out below and above the glass-transition temperature, to investigate the influence of the physical state on the specific heat C_p, whereby a value 50% greater than that previously measured was found in the second case.

The simulation of the FP process was carried out using Matlab® software (The MathWorks, Natick, MA) on a Pentium 4–based personal computer.

The experimental verification of the model was performed in a small-scale cylindrical reactor (ID, 14 mm; length, 200 mm). Four thermocouples connected to a data-acquisition system were used to monitor the polymerization front advancement along the tube's axial direction and to measure the temperature of the reacting system during the process time: that is, three of them were put in contact with the external wall of the reactor at 22.2, 40.4, and 58.2 mm from the top end of the tube, respectively; the fourth one was placed inside the reactor along its central axis to measure the actual temperature reached by the front. The reaction was triggered using a small block of steel warmed up to 200°C. The block was maintained in contact with the resin surface at the top end of the tube for 60 s. Fronts were descending.

RESULTS AND DISCUSSION

Experimental study

From the temperature profiles reported in Figure 1 it was possible to calculate the instant at which the hot front passed through. This time was calculated to correspond with the highest rate of temperature increase, evidenced by the peak of the derivative curves shown in Figure 1(b), corresponding to the three points along the reactor (see experimental section). The position of the front, calculated with the above procedure, is shown in Figure 2. As can be seen, the polymerization front propagates at constant speed. This a typical feature found in those FP processes where a steady state has been reached, and is attributed to the equilibrium between the heat dissipated and that exploited by the reaction to self-sustain. Furthermore, such linear behavior is generally found when a pure FP is occurring, which means that no spontaneous polymerization is simultaneously taking place. This latter finding is also confirmed by the flat part of the curves registered by the thermocouples before being crossed by the incoming front (Fig. 3).

Reaction kinetics

The first step performed toward the simulation of the entire process was the selection of a mathematical model able to describe the reaction kinetics of the chosen resin system, to relate the time and the tem-

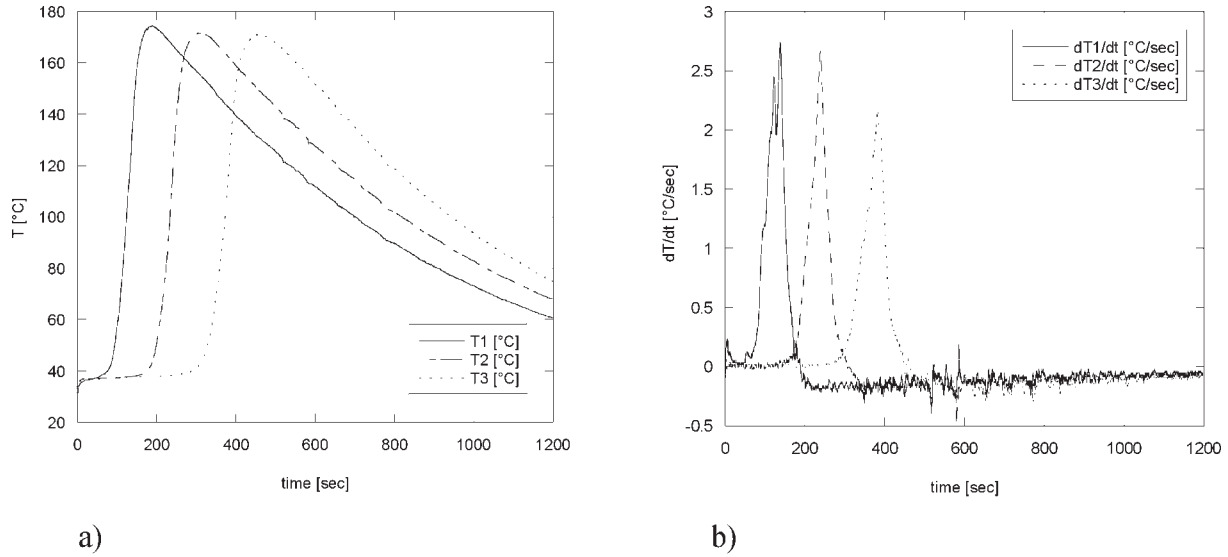

Figure 1 (a) Temperature profiles of the three thermocouples fixed to the wall of the test tube reordered during the experiment. (b) Time derivative of the temperature profiles reordered from the three thermocouples fixed to the wall of the test tube.

perature evolution in the reactor to the heat produced by the reaction itself.

From the DSC tests, the degree of cure was defined as[24]

$$\alpha = \frac{H(t)}{H_{\text{tot}}} \tag{1}$$

where $H(t)$ is the heat produced during the cure at a given time t, and H_{tot} is the total heat of reaction developed by the resin to be fully cured. For all the isotherms, the heat released by the resin was lower than that produced during the dynamic tests, showing that the reaction was controlled by diffusion. Therefore, the maximum isothermal degree of cure $\alpha_{\max}$ was less than 1 and in all cases, a linear dependency[23] of $\alpha_{\max}$ on the process cure temperature (see Fig. 4) was observed.

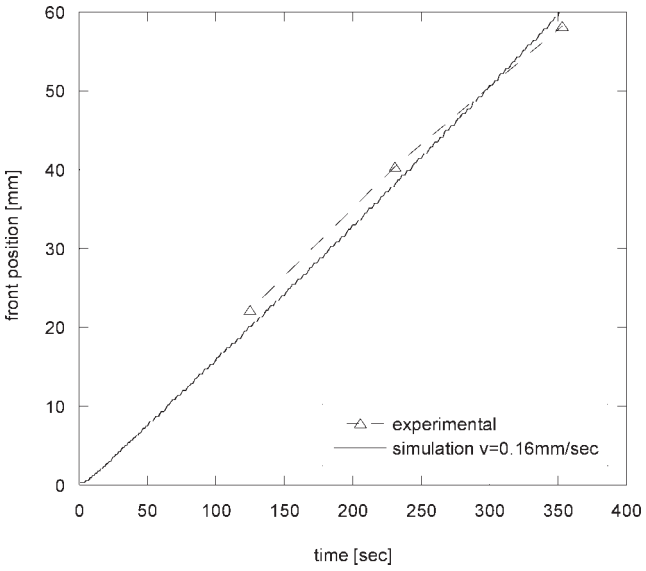

Figure 2 Experimental results compared with the prediction of the model for front advancement along an axial direction. In the simulation, a C_p of 2230 J kg^{-1} K^{-1} was used.

On the basis of the considerations previously made regarding the role played by $\alpha_{\max}$ and from the shape of the curves related to $d\alpha/dt$, the phenomenological model represented by eq. (2) was adopted to describe the cure process for the epoxy system:

$$\frac{d\alpha}{dt} = (k_1 + k_2\alpha^m)(\alpha_{\max} - \alpha)^n \tag{2}$$

where

$$k_1 = k_{01} \exp\left(-\frac{E_{\text{att1}}}{RT}\right)$$

$$k_2 = k_{02} \exp\left(-\frac{E_{\text{att2}}}{RT}\right)$$

$$\alpha_{\max} = pT + q$$

where k_{01} and k_{02} are kinetic constants, E_{att1} and E_{att2} are activation energies for the polymerization process, and m and n represent the reaction order.

Because eq. (2) is nonlinear, the determination of the parameters necessary to describe the problem is quite complicated[25]; therefore a genetic algorithm to fit the

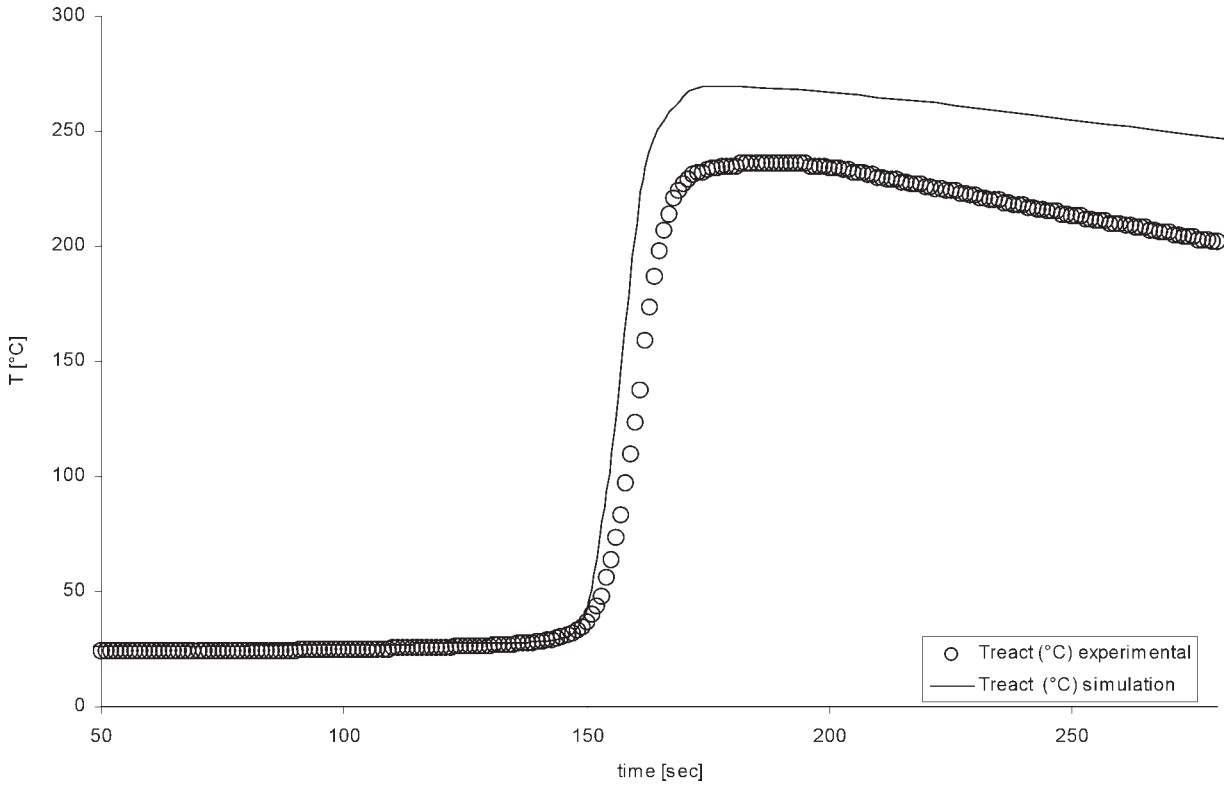

Figure 3 Temperature profiles of the thermocouple lying on the axis of the cylinder reordered during the experiment.

experimental data[26,27] was used. As shown in Figure 5, a good agreement between the experimental data and the proposed model was obtained. The parameters describing the kinetic equation are summarized in Table II.

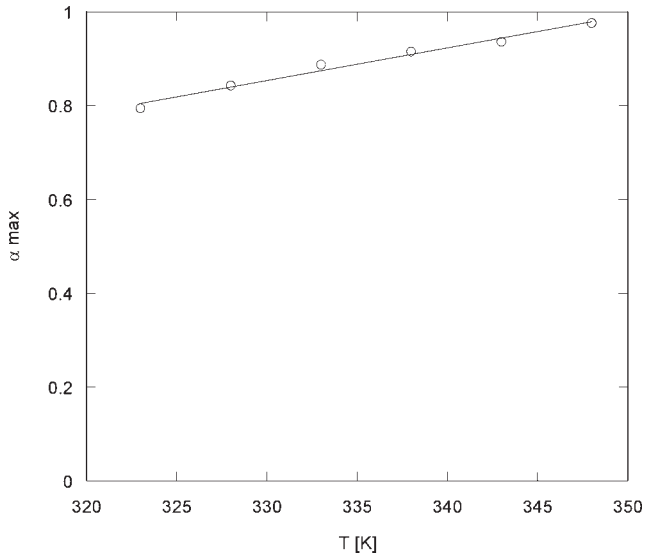

Figure 4 α_{max} plotted versus the isothermal cure temperature T. Experimental points were well fitted by a linear regression.

Numerical modeling

The front advancement phenomenon was mathematically modeled to better understand it and to provide the basis for an accurate process simulation. The geometry of the reactor chosen for the mathematical model was cylindrical and its dimensions are the same as those of the experiment (ID, 14 mm; length, 200 mm).

The system of equations that describes the problem includes the heat-exchange equation and the description of the cure kinetics of the resin:

$$\begin{cases} \nabla\left(k\,\nabla\,T\right) + \dot{H} = \rho C_p \dfrac{\partial T}{\partial t} \\ \dfrac{d\alpha}{dt} = K_0 \exp\left(-\dfrac{E_{\text{att}}}{\text{RT}}\right) f(\alpha) \end{cases} \tag{3}$$

where α is the degree of cure, E_{att} is the activation energy of the crosslinking reaction, and R is the gas constant. This system of equations is coupled by the relation that links the rate of heat generation $\dot{H}$ with $d\alpha/dt$ that is the time rate of reaction, expressed in the following equation:

$$\dot{H} = \rho H_{\text{tot}} \frac{d\alpha}{dt} \tag{4}$$

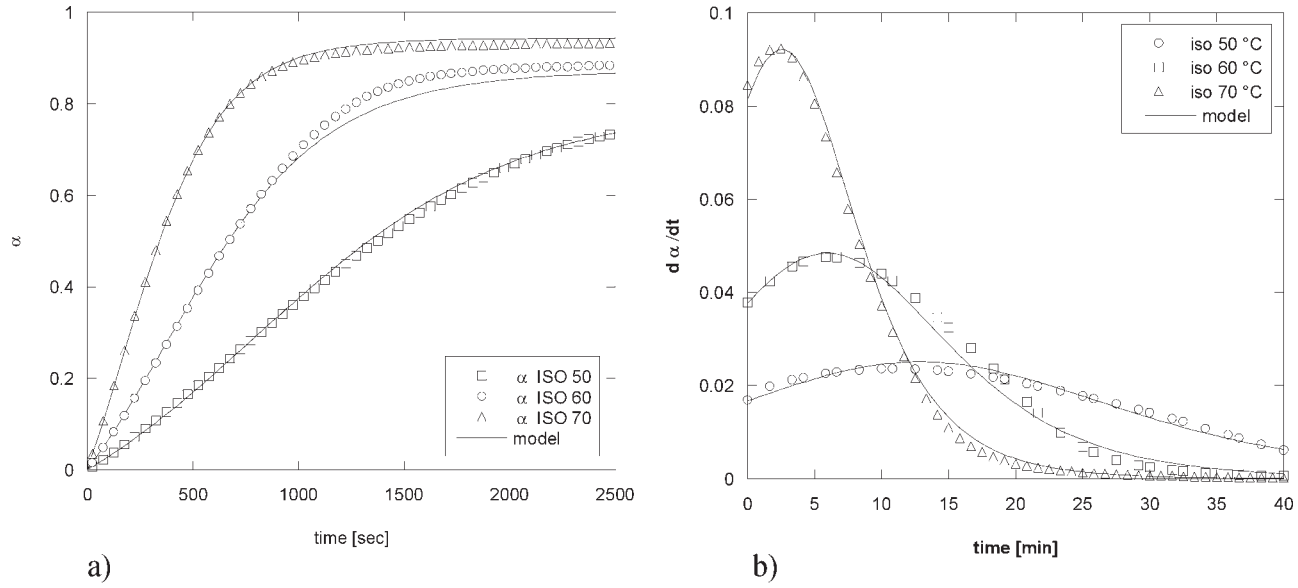

Figure 5 Experimental results compared with the prediction of the model: (a): α versus time, b): $d\alpha/dt$ versus time.

where H_{tot} is the total heat of reaction.

A finite-difference method was used to solve the system of eq. (3) within the model domain. Two different cases were analyzed. First, the model was developed by considering the cylinder to be adiabatic during the front propagation. Because the reaction is initiated by heating the whole upper surface of the reaction mixture, the heat-exchange equation needs to be solved only along the axial direction. Indeed, for reasons of symmetry no heat exchange in the radial direction, nor along any angular direction, is expected. Consequently, the temperature profile and the degree of cure are functions of only the axial direction. A one-dimensional model was thus used to analyze this particular case. The thermal-exchange equation was solved using the implicit backward time–centered space method.[28] The boundary condition applied was that no heat exchange would occur during the entire process cycle through the walls and the bottom end of the cylinder. The latter condition is expressed by

$$\frac{dT}{dz} = 0 \tag{5}$$

The top end was set at a fixed temperature for a time period long enough to simulate the ignition of the reaction, after which the system was considered adiabatic for the rest of the process. To obtain a more flexible model, the entire problem was adimensionalized using dimensionless variables, and the temperature, time, and axis coordinates are expressed in the following equations, respectively:

$$\theta = \frac{T - T_{ref}}{T - T_0} \tag{6}$$

$$t^* = \frac{t}{t_{gel}} \tag{7}$$

$$z^* = \frac{z}{L} \tag{8}$$

where T_{ref} is the reference temperature, which for this study was set as T_{trig}; t_{gel} is a reference time representing the isothermal gel time for the resin; and L is the reactor length.

By substituting eqs. (5)–(8) in eq. (3), the problem is described by

$$\begin{cases} \mathrm{De}\nabla^2\theta + \mathrm{St}\dfrac{d\alpha}{dt^*} = \dfrac{\partial\theta}{\partial t^*} \\ \dfrac{d\alpha}{dt} = K_0 \exp\left(-\dfrac{E_{att1}}{RT}\right) f(\alpha) \end{cases} \tag{9}$$

TABLE II
Kinetic Parameters of the Phenomenological Model Found for the Studied System

Parameter	Value
$\ln(k_{01})$, $\ln(1/\mathrm{min})$	20.2
E_{att1}, kJ/mol	64,735
$\ln(k_{02})$, $\ln(1/\mathrm{min})$	9.5
E_{att2}, kJ/mol	31,561
m	1
n	1.07
p, 1/°C	6.96E-3
q	4.57E-1

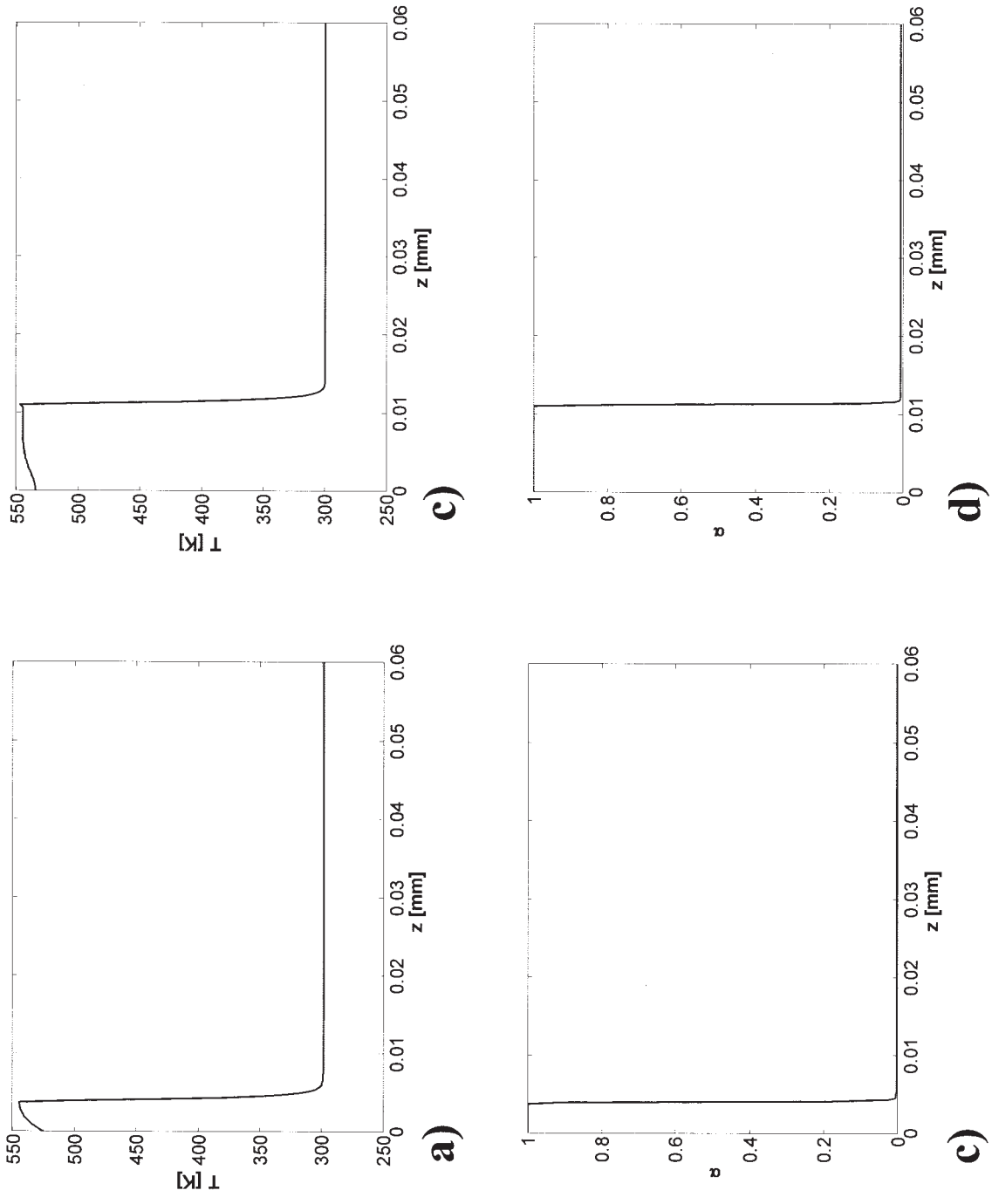

Figure 6 Temperature distribution in the cylinder obtained using a one-dimensional model: (a) after 60 s and (b) after 120 s. Distribution of the degree of cure along the cylinder axis predicted by a one-dimensional model: (c) after 60 s and (d) after 120 s.

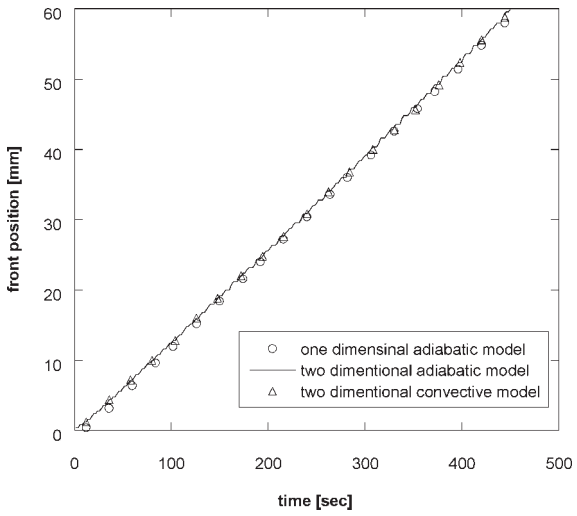

Figure 7 Front advancement along the cylinder axis as a function of time: comparison of the results obtained from the one-dimensional adiabatic model and from the two-dimensional adiabatic and with convective boundaries, respectively.

where De and St are the Deborah and Stefan adimensional numbers, respectively,.[29] In particular, the Deborah number provides an indication of the ratio between the heat diffused by conduction and the heat retained by volume, expressed as

$$\mathrm{De} = \frac{kt_{\mathrm{gel}}}{\rho C_p L^2} \tag{10}$$

whereas the Stefan number represents the ratio between the total heat produced by the reaction, H_{tot}, and the heat necessary to increase the volume temperature, expressed as

$$\mathrm{St} = \frac{H_{\mathrm{tot}}}{C_p(T_{\mathrm{ref}} - T_0)} \tag{11}$$

The thermal problem was solved at each time step n, leading to the temperature distribution for each j point of the grid along the axis of the cylinder. The Thomas algorithm was used to solve the linear system obtained from the finite-difference formulation.[28] The resulting temperature array T_n^j was used to evaluate the evolution of the degree of cure at each point of the grid using a Runge–Kutta 4–5°-order method. From the $n+1$ newly calculated $\alpha zsxj$, it was possible to obtain the rate of heat generation to be included in the equations needed to solve the thermal problem at the time step $n + 1$ for each point of the grid. The entire process was iterated until the desired time was reached. The resin properties used for the simulation are reported in Tables I and II and were experimentally calculated. The distribution of temperature and the degree of cure within the domain of the reactor after the triggering time and after 120 s are presented in Figure 6. The results show that, starting from the warmed end of the reactor, a reactive hot front was created that advanced along the axial direction of the cylinder at a constant speed, as shown in Figure 7. Using the model, it was possible to evaluate the influence of various parameters on the velocity of the propagating front. Figure 8(a) and (b) show the influence of the resin thermal conductivity k and of the total heat of reaction H_{tot} on the front velocity, respectively.

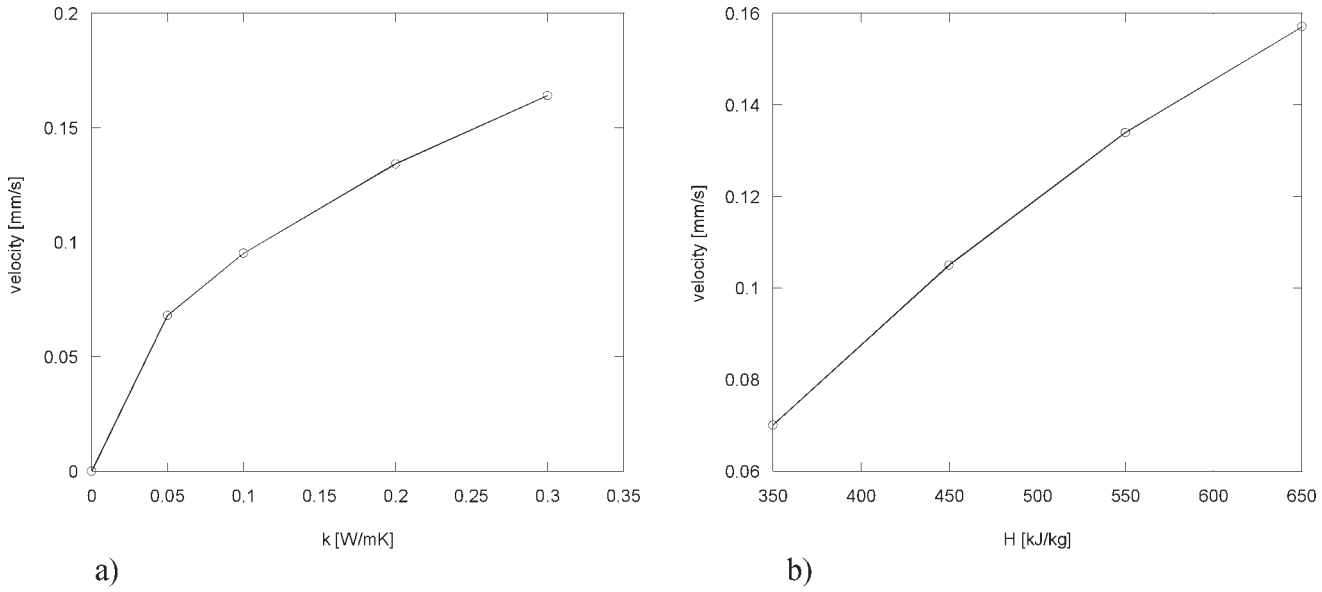

Figure 8 (a) Influence of resin thermal conductivity on the speed of the reactive front; (b) influence of the total heat of reaction of the resin on the speed of the reactive front.

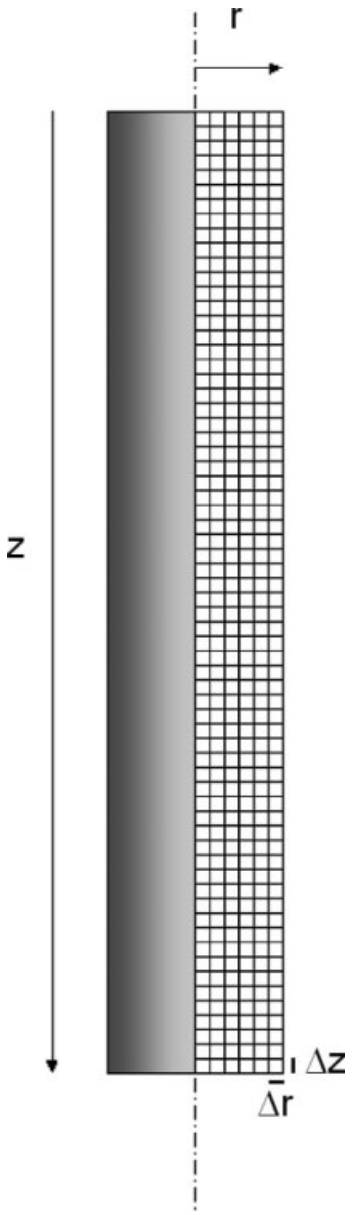

Figure 9 Finite-difference grid considered for the two-dimensional model.

To consider the influence of the adiabatic boundary conditions, a three-dimensional finite-difference model of the reactor provides more accurate indications and was therefore developed.

The cylindrical geometry of the system together with the symmetrical boundary conditions imply that the variables are not dependent on the angular direction and thus the problem turns out to be two-dimensional. In Figure 9 the calculation domain is shown; from the above assumptions it is clear that it is possible to analyze only a portion of the entire geometry. The model equations were solved using the alternate direction implicit method[28] to maximize the computational efficiency of the model. For the determination of the derivatives, this approach uses a virtual intermediate time step, indicated by the superscript $n + (1/2)$. The entire integration procedure at the time step $(n + 1)$, corresponding to a generic point (i, j), is summarized in the following equations:

$$\mathrm{De}\left(\frac{\theta_{i-1,j}^{n+(1/2)} - 2\theta_{i,j}^{n+(1/2)} + \theta_{i+1,j}^{n+(1/2)}}{(\Delta z^*)^2} + \nabla_r^2\theta_{i,j}^n\right) + \mathrm{St}\,\frac{\partial\alpha}{\partial t} = \frac{\theta_{i,j}^{n+(1/2)} - \theta_{i,j}^n}{\Delta t^*} \quad (12)$$

$$\mathrm{De}\left(\nabla_z^2\theta_{i,j}^{n+(1/2)} + \frac{\theta_{i,j-1}^{n+1} - 2\theta_{i,j}^{n+1} + \theta_{i,j+1}^{n+1}}{(\Delta r^*)^2} + \frac{\theta_{i,j-1}^{n+1} - \theta_{i,j+1}^{n+1}}{(\Delta r^*)^2}\right) + \mathrm{St}\,\frac{\partial\alpha}{\partial t} = \frac{\theta_{i,j}^{n+1} - \theta_{i,j}^{n+(1/2)}}{\Delta t^*} \quad (13)$$

Boundary conditions (BC) imposed no heat flux in the radial direction for those points of the grid lying on the axis of the cylinder. On the external surfaces convective heat exchange was considered, and thus the BC are described by the following equation:

$$\left(\frac{dT}{dz}\right)_{i,j} = \frac{h}{k}\,(T_{i,j} - T_{\mathrm{air}}) \quad (14)$$

In the reaction ignition, in the side region of interest, the same boundary conditions developed for the one-dimensional model were used except for the fact that, after the ignition time t_{trig}, the boundary was considered exposed to thermal convection instead of considering it as an adiabatic boundary.

To validate the consistency of the results obtained by the two different approaches, the one-dimensional and the two-dimensional models were compared by simulating an adiabatic reactor. The result of the comparison in terms of front advancement versus time is summarized in Figure 7.

With the two-dimensional model and using an appropriate value of the film coefficient h,[30] it was possible to study the process in the case where the reactor was exposed to natural convection. The parameters used in these simulations are summarized in Table III and the relationship between the front position and the time along the axis of the cylinder

TABLE III
Parameters Governing Convection Thermal Exchange Used in the Two-Dimensional Model

Parameter	Value
Film coefficient h, $\mathrm{W/m^{-2}/K^{-1}}$	6.85
Air temperature, °C	25

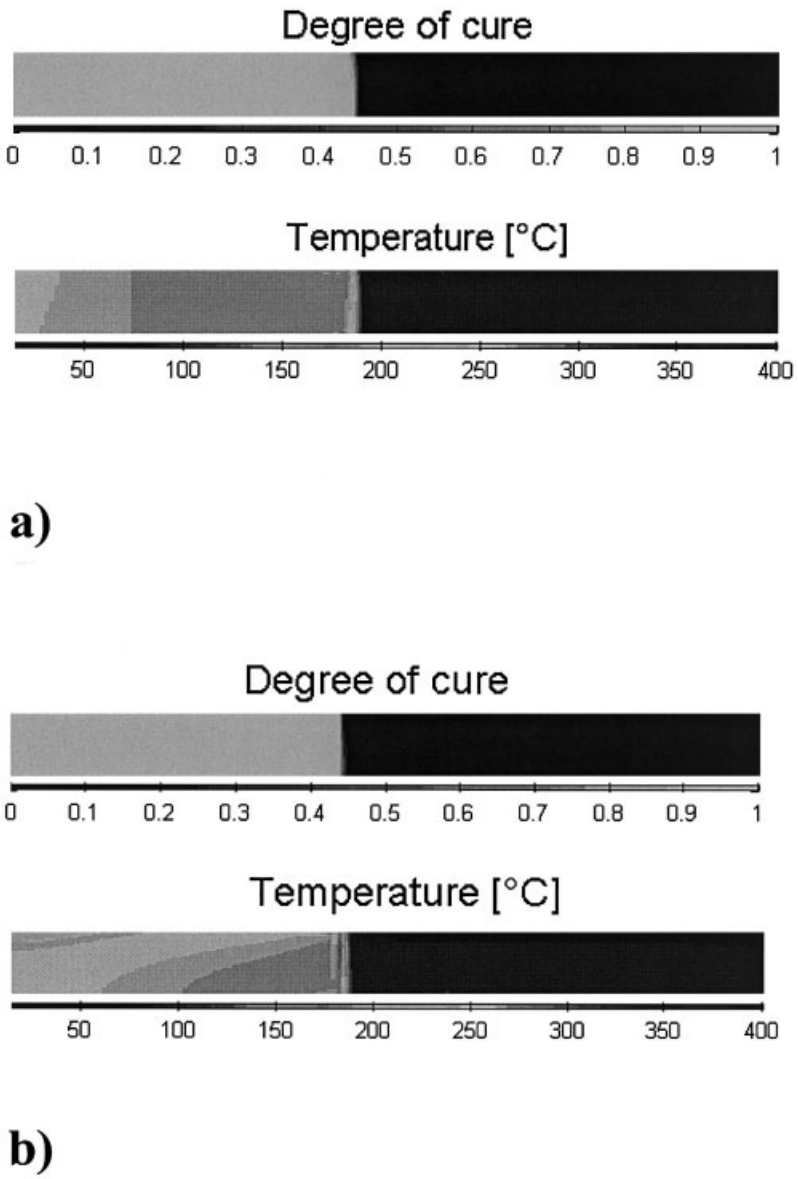

Figure 10 Temperature profile and degree of cure in the reactor after 200 s: (a) in case of adiabatic boundaries; (b) in case of natural convection at the boundaries.

is shown in Figure 7, where the results obtained are compared with those of the two-dimensional adiabatic model and the one-dimensional adiabatic model. As one can see, there is no appreciable difference in terms of velocity of the front between the case of natural and that of adiabatic convection, meaning that the BC tested have no effect on front propagation. Conversely, a strong influence of the BC was observed on temperature distribution. In Figure 10(a) and (b) the temperature and the degree of cure distributions in the reactor, taken 200 s after the reaction onset, are compared for the adiabatic and the convective BC. For the adiabatic model, once the front passed through a transversal section of the reactor, the temperature remained constant for the rest of the process. This happened because there was no opportunity for thermal exchange in the transverse direction. The heat flux along the front propagation direction was also driven by the sudden ignition of the monomer lying close to the reactive front that rapidly heated the resin to the same temperature of the zones previously simulated in the reaction.

In the case of the model with convective BC, the reaction was promoted by a hot reaction wave moving along the reactor, and once the hot reactive front passed, the temperature was lowered by thermal exchange toward the reactor walls. Despite the results

obtained in terms of temperature for the two-dimensional models with adiabatic or convective BC, the cure degree distribution after 200 s was identical in both cases. Indeed, the degree of cure was influenced by the front temperature and not by the thermal evolution of the polymer after the front passed through it; therefore in both cases, the same evolution for the reaction degree was observed.

To validate the simulation program, the experiments performed in the test tube were simulated. The resin properties used as input were obtained by the characterization work (Tables I and II). The value of the specific heat of the resin was measured at room temperature. In Figure 2, the results of the simulation in terms of front position with respect to time are compared with the experimental ones. As shown by the graph, the front velocity predicted by the model concurs with the experimental measurements. The thermal history measured by the thermocouple on the axis of the cylinder was also simulated. The results of the simulation are shown in Figure 3. As one can see, the maximum temperature predicted by the model was slightly higher than that measured experimentally. This result can be attributed to the fact that, to lower the calculation time, the value of the specific heat was considered constant in the model. Conversely, the good correlation between the experimental data and the model results on front position confirms the validity of the simulation program.

CONCLUSIONS

Finite-difference models to simulate the front polymerization process for a cylindrical reactor have been developed. First, a one-dimensional model, able to describe the process in a tube with no thermal exchange with the surroundings, was developed. An epoxy–amine thermoset system was used as the model system. It was completely characterized and its cure kinetics was modeled using a phenomenological approach. The kinetic parameters were found using a genetic algorithm to fit the experimental data with the theoretical model. Simulations were carried out taking into consideration the chemophysical properties of the characterized resin. From the calculations, the formation of a reactive front, advancing in the monomer at a constant speed, was predicted. The influence of the chemical and physical properties of the resin on the front advancement was also investigated, showing that this parameter is strongly influenced by thermal conductivity and by the total reaction heat. Second, a two-dimensional model was developed to study the influence of the boundary conditions on the process evolution when convective heat exchange at the wall of the cylindrical reactor is considered.

The results showed that heat exchange at the boundary has no effect on the front velocity, whereas it strongly influences the thermal history of the resin. Using a glass test tube, a simple experimental reactor was built. Front propagation along the axial direction was then promoted, the front position was monitored using three thermocouples fixed to the lateral surface of the glass tube, and temperature evolution was monitored during the process time.

The thermal history of the resin inside the reactor was also measured using a thermocouple placed on the axis of the cylindrical reactor.

Front velocity predicted by the model concurred with the experimental measurements. A good correlation for the thermal history of the resin during process evolution was also found, even if the strong dependency of the specific heat of the resin on temperature, which was not considered in the model, influenced the model predictions.

References

1. Begishev, V. P.; Volpert, V. A.; Davtyan, S. P.; Malkin, A. Y. Dokl Akad Nauk SSSR 1973, 208, 892.
2. Goldfeder, P. M.; Volpert, V. A.; Ilyashenko, V. M.; Khan, A. M.; Pojman, J. A.; Solovyov, S. E. J Phys Chem B 1997, 101, 3474.
3. Davtyan, S. P.; Arutyunyan, K. A.; Shkadinskii, K. G.; Rozenberg, B. A.; Yeniko-lopyan, N. S. Polym Sci USSR 1978, 19, 3149.
4. Korotkov, V. N.; Chekanov, Y. A.; Rozenberg, B. A. Compos Sci Technol 1993, 47, 383.
5. White, S. R.; Kim, C. J Reinf Plast Comp 1993, 12, 520.
6. Chekanov, Y.; Arrington, D.; Brust, G.; Pojman, J. A. J Appl Polym Sci 1997, 66, 1209.
7. Mariani, A.; Bidali, S.; Fiori, S.; Sangermano, M.; Malucelli, G.; Bongiovanni, R.; Priola, A. J Polym Sci Polym Chem Ed 2004, 42, 2066.
8. Pojman, J. A.; Elcan, W.; Khan, A. M.; Mathias, L. J Polym Sci Part A: Polym Chem 1997, 35, 227.
9. Fiori, S.; Mariani, A.; Ricco, L.; Russo, S. Macromolecules 2003, 36, 6539.
10. Mariani, A.; Bidali, S.; Fiori, S.; Malucelli, G.; Sanna, E. e-Polymers 2003, 44, 1.
11. Mariani, A.; Fiori, S.; Chekanov, Y.; Pojman, J. A. Macromolecules 2001, 34, 2674.
12. Fiori, S.; Mariani, A.; Ricco, L.; Russo, S. e-Polymers 2002, 029, 1.
13. Fiori, S.; Malucelli, G.; Mariani, A.; Ricco, L.; Casazza, E. e-Polymers 2002, 057, 1.
14. Fiori, S.; Mariani, A.; Bidali, S.; Malucelli, G. e-Polymers 2004, 01, 1.
15. Pojman, J. A.; Varisli, B.; Perryman, A.; Edwards, C.; Hoyle, C. Macromolecules 2004, 37, 691.
16. Bidali, S.; Fiori, S.; Malucelli, G.; Mariani, A. e-Polymers 2003, 060, 1.
17. Pojman, J. A.; Curtis, G.; Ilyashenko, V. M. J Am Chem Soc 1996, 118, 3783.
18. Pojman, J. A.; Ilyashenko, V. M.; Khan, A. M. J Chem Soc Faraday Trans 1996, 92, 2825.
19. Pojman, J. A.; Elcan, W.; Khan, A. M.; Mathias, L. J Polym Sci Part A: Polym Chem 1997, 35, 227.

20. Fortenberry, D. I.; Pojman, J. A. J Polym Sci Part A: Polym Chem 2000, 38, 1129.
21. Apostolo, M.; Tredici, A.; Morbidelli, M.; Varma, A. J Polym Sci Part A: Polym Chem 1997, 35, 1047.
22. Spade, C. A.; Volpert, V. A. Chem Eng Sci 2000, 55, 641.
23. Kenny, J. M.; Trivisano, A. Polym Eng Sci 1991, 31, 1426.
24. Turi, A. Thermal Characterization of Polymeric Materials; Academic Press: San Diego, CA, 1997.
25. Kenny, J. M. J Appl Polym Sci 1994, 51, 761.
26. Brunetti, A. Comput Phys Commun 2000, 124, 204.
27. Nikitas, P.; Papageorgiou, A. Comput Phys Commun 2001, 141, 225.
28. Hoffman, J. D. Numerical Methods for Engineers and Scientists; Mc-Graw Hill: New York, 1993.
29. Kenny, J. M.; Apicella, A.; Nicolais, L. Polym Eng Sci 1989, 29, 973.
30. Perry, R. H.; Green, D. W. Perry's Chemical Engineers' Handbook; Mc-Graw Hill: New York, 1997.